1-1-2017

Fate and Impacts of Triclosan, Sulfamethoxazole, and 17β-estradiol during Nutrient Recovery via ion Exchange and Struvite Precipitation

Yiran Tong
Marquette University

Patrick J. McNamara
Marquette University, patrick.mcnamara@marquette.edu

Brooke K. Mayer
Marquette University, Brooke.Mayer@marquette.edu

Accepted version. *Environmental Science: Water Research & Technology* (2017). DOI.

Fate and Impacts of Triclosan, Sulfamethoxazole, and 17β-Estradiol during Nutrient Recovery via Ion Exchange and Struvite Precipitation

Yiran Tong[a], Patrick J. McNamara[a], Brooke K. Mayer[a*]
[a] Department of Civil, Construction and Environmental Engineering, Marquette University, 1637 W. Wisconsin Ave., Milwaukee, WI 53233, USA

*Corresponding author: Email:Brooke.Mayer@marquette.edu Phone: 414-288-2161

Abstract

Increasing emphasis on resource recovery from wastewater highlights the importance of capturing valuable products, e.g., nutrients such as nitrogen and phosphorus, while removing contaminants, e.g., organic micropollutants. The objective of this research was to evaluate the fate of the micropollutants triclosan (present as a mixture of neutral and anionic species at neutral pH), 17β-estradiol (neutral at neutral pH), and sulfamethoxazole (anionic at neutral pH) during nutrient recovery using ion exchange-precipitation. Adsorption of the three micropollutants to the phosphate-selective ion exchange resins LayneRT and DOW-HFO-Cu ranged from 54% to 88%. The micropollutants did not sorb to the ammonium-selective resin, clinoptilolite. The presence of the micropollutants reduced kinetics of nutrient exchange rates onto ion exchangers. However, the micropollutants did not interfere with nutrient capacity on the ion exchangers, likely due to the low concentration of micropollutants and potentially different mechanisms of adsorption (i.e., coulombic and non-coulombic attractions for micropollutants) compared to the target ions. Less than half of the micropollutants that sorbed to the phosphate exchangers were released with phosphate ions during regeneration. Concentrations of NaOH and NaCl in regeneration solutions did not statistically correlate with the amount of desorbed micropollutants, which may be attributed to the complexity of micropollutants' binding mechanisms with ion exchangers. Triclosan, the most hydrophobic of the three micropollutants studied, adsorbed to the resins to the greatest extent and demonstrated the lowest desorption rates during regeneration. Batch struvite precipitation tests revealed that the micropollutants were not enmeshed in precipitated struvite crystals nor sorbed during crystallization, indicating that the struvite product was free of triclosan, 17β-estradiol, and sulfamethoxazole.

Introduction

Water resource recovery facilities (WRRFs) are inextricably linked to the food, energy, and water nexus as they provide a centralized opportunity to recover energy, e.g., as methane; produce high-quality treated water; and recover valuable products, e.g., for use as agricultural fertilizers or soil amendments[1]. Anaerobic treatments such as anaerobic membrane bioreactors (AnMBRs) for secondary treatment and anaerobic digestion (AD) for solids treatment produce methane, which can offset some energy requirements for WRRFs. Furthermore, AnMBRs do not require aeration and could be a more sustainable alternative to conventional activated sludge processes [2–5]. Additionally, anaerobic processes offer an opportunity for downstream nutrient recovery and thus an option to produce and recover a valuable product instead of using energy to convert nutrients to a wasted product (e.g., as an off-gas).

The effluent from anaerobic processes usually contains high ammonia nitrogen (NH_4-N) and inorganic phosphate (PO_4-P) [2,4]. Accordingly, additional nutrient removal technologies may be needed to treat anaerobic effluent to meet increasingly stringent nutrient discharge regulations [6]. While excess phosphorus and nitrogen in environmental waters causes eutrophication [7], insufficient nutrient availability is also a concern for agriculture [8]. Depleting reserves of mined phosphate, together with the energy-intensive nature of Haber-Bosch nitrogen fixation, could limit global food production [9,10]. Anaerobic effluent, as a reservoir of nutrients, is a resource from which to recover nitrogen and phosphorus in the form of a solid fertilizer product that can help to close anthropogenic nutrient loops by supplementing nonrenewable phosphate mining and energy-intensive atmospheric nitrogen fixation [11].

Wastewater contains a host of inherently valuable constituents including energy and nutrients, but it also contains a mixture of micropollutants that pose potential adverse ecological health impacts [12]. For example, triclosan (TCS) is an antimicrobial agent used in a variety of consumer products, and can select for antibiotic resistance in engineered and natural systems [13–16]. 17β-estradiol (E2) is a natural hormone that is linked to fish feminization near treatment plant outfalls [17]. Sulfamethoxazole (SMX) is one of the most popularly prescribed sulfonamide antibiotics and can affect nutrient cycling in microbial communities [18,19]. WRRFs were not specifically designed to remove micropollutants, and anaerobic processes are often worse at removing micropollutants compared to aerobic processes. For instance, Samaras et al. (2013) reported approximately 20±35% removal of TCS via biotransformation using AD [20]. Studies on endocrine disruptors such as estrone (E1), E2 and 17α-ethynylestradiol (EE2) revealed that AD and AnMBRs offered poor biotransformation of these compounds [21–23]. SMX had variable biological

transformation in AD and AnMBR systems, ranging from 41.9% to 99% [23–25]. If valuable products such as treated water and nutrients are to be recovered from anaerobic effluents, it is important to understand the fate of micropollutants to ensure that they are not enriched in the WRRF products. This study focused on the impact and fate of TCS, E2 and SMX during nutrient recovery because of the potential presence of these micropollutants in anaerobic effluent and their different physicochemical properties (molecular details of which are included in the Supplemental Information [SI], S1).

One option for removing and recovering nutrients is ion exchange-precipitation. In this process, nutrient-selective materials are used to extract and concentrate nitrogen and phosphorus via ion exchange and subsequent regeneration followed by precipitation of nutrient-rich solid fertilizer products, e.g., struvite ($MgNH_4PO_4$). Clinoptilolite is a natural zeolite that effectively exchanges ammonium ions [26]. In wastewater, phosphorus is most commonly present in the HPO_4^{2-} and $H_2PO_4^-$ forms [27]. These orthophosphate species can exhibit strong ligand sorption to polyvalent metals such as Fe(III) and Cu(II) by forming inner-sphere complexes [28,29]. Therefore, polymeric anion exchangers are usually impregnated with metal salts to selectively exchange orthophosphate. After removal, nutrients are concentrated during ion exchange regeneration, thereby facilitating precipitation of nutrient-rich solids that can be used as fertilizer. Controlled struvite precipitation has been studied in mainstream and side-stream wastewater (direct precipitation) [30–32] and in membrane-concentrated streams and ion exchange regeneration brines (indirect precipitation) [31,33]. Compared to direct precipitation, indirect precipitation is more favorable for producing a high purity mineral and easier operational control [31]. However, organic micropollutants such as tetracycline and quinolones have been detected in struvite produced from digester filtrate and urine [34,35]. Thus, if valuable fertilizer is recovered from anaerobic effluents, it is essential to thoroughly assess the potential for co-concentration of residual micropollutants along with nutrients.

The objective of this work was to evaluate the fate of the micropollutants TCS, E2, and SMX during ammonium and phosphate ion exchange-regeneration and struvite precipitation. Batch experiments were conducted to specifically determine: a) the impact of micropollutants on nutrient exchange reaction rates, capacities and desorption, b) the fate of the micropollutants during ion exchange-regeneration-precipitation, and c) micropollutants' impact and fate during ion exchange-regeneration in actual anaerobic filtrate.

Materials and Methods

Ion exchangers

LayneRT and DOW-HFO-Cu were evaluated as phosphate-selective ion exchangers [29,36]. LayneRT (Layne Christensen, The Woodlands, TX) is a 300 - 1200 µm particle size ready-to-purchase hybrid anion exchange resin consisting of hydrated ferric oxide (HFO) nanoparticles impregnated in a strong base anion exchange polymer [29]. DOWEX M4195 (DOW Chemical Company, Midland, MI) was used as the base resin for producing functional DOW-HFO-Cu resin by immobilizing Cu(II) and HFO, which provide ligand bonding with HPO_4^{2-} and $H_2PO_4^-$, onto the 300 - 850 µm particle size polymer, in accordance with Sengupta and Pandit 's protocol [29]. Clinoptilolite, a natural zeolite, was used as a selective ammonium exchanger (420 – 1410 µm particle size). Clinoptilolite (St. Cloud Mining, Winston, NM, 14X40 mesh) was pre-conditioned with 1% NaCl solution and rinsed with de-ionized water.

Ion exchanger characterization

Characterization of ion exchangers was performed to better elucidate the interactions between the dissolved chemicals and the ion exchangers. Ion exchanger surface area and pore size were measured using a Brunauer–Emmett–Teller (BET) surface analysis instrument (NOVA 4200e, Quantachrome Instruments, Boynton Beach, FL). The surface charge of the materials was determined using a Malvern Zetasizer Nano S (Malvern Instruments Ltd, Malvern, UK). The ion exchangers' surface element composition was observed via JEOL JSM-6510LV SEM (JEOL USA, Inc., Peabody, MA) with an energy-dispersive X-ray (EDX) detector at an accelerating voltage of 10 kV.

Ion exchange and regeneration batch experiments

Batch ion exchange tests were conducted to determine if micropollutants would be co-captured with nutrient ions. These tests were performed in feed water with 40 mg-N/L as NH_4Cl and 5 mg-P/L as K_2HPO_4 [33] to mimic plausible nutrient levels in anaerobic effluents [2]. The feed water was prepared by dissolving 300±50 µg/L each of TCS, E2 and SMX in HPLC-grade methanol. The volumetric ratio of methanol stock to water was below 0.5% to negate co-solvent effects [37]. The spiked micropollutant concentrations were higher than in actual anaerobic effluents [23,24] so that reaction rates and adsorption capacities could be determined via liquid chromatography-mass spectrometry (LC-MS; detection limits were in the low µg/L range). The pH of feed water was adjusted to 7 with NaOH.

For ion exchange tests, 50 mL feed water was added to 60 mL serum bottles. Each bottle contained either 0.25 g clinoptilolite, 0.05 g LayneRT, or 0.05 g DOW-HFO-Cu resin

(higher levels of clinoptilolite were added based on higher ammonium concentrations). The bottles were mixed on a rotating tumbler for 4 days as preliminary tests demonstrated this time was sufficient time to achieve equilibrium. For kinetic tests, periodic samples were collected for four days, as shown in Figures 1 and 2. Nutrient exchange typically achieved equilibrium in less than one day and micropollutants adsorption typically achieved equilibrium within two days (<5% change in concentrations).

Ion exchange isotherm tests were conducted to assess potential interference with nutrient capture caused by micropollutants. For these tests, 50 mL of feed water were added to 60 mL serum bottles. The amount of ion exchanger in each bottle varied: 0.01, 0.02, 0.03, 0.04, or 0.05 g DOW-HFO-Cu or LayneRT; 0.01, 0.05, 0.1, 0.2, or 0.5 g clinoptilolite. Samples were analyzed at time zero and after 4 days.

Ion exchange regeneration tests were conducted to determine if the micropollutants that were adsorbed on the ion exchangers would be released during subsequent regeneration. All ion exchangers were regenerated using brine solutions with high levels of Na^+, Cl^- and OH^- [33,38]. For clinoptilolite, the regeneration brine was fixed at 8% NaCl [33]. The concentrations of NaCl and NaOH in phosphate exchanger regeneration brine were varied to study their impact on phosphate and micropollutant recovery (S2, Tables S2-S5). Differences in recoveries as a function of regeneration solution could enable process optimization to elicit greater desorption of nutrients and less desorption of micropollutants. The regeneration brine for LayneRT ranged from 0 to 2% NaCl and 0 to 2% NaOH. The regeneration brine for DOW-HFO-Cu ranged from 0 to 2.5% NaCl and 0 to 2% NaOH [39]. The pH of all regeneration brines was 12 to 14. Ion exchange tests were initially performed in 250 mL water in 500 mL Erlenmeyer flasks. The amount of ion exchanger added to each flask was fixed at 1.25 g clinoptilolite or 0.25 g DOW or LayneRT resin. After completing the 4-day ion exchange period, the flasks were decanted and 150 mL NaCl+NaOH regeneration solution was added. Regeneration lasted for 4 hours, in accordance with previous equilibrium tests [33]. Samples were collected for nutrient and micropollutant analysis from the feed water, after ion exchange, and after regeneration.

Tests in actual anaerobic wastewater filtrate

A filtrate sample from a belt filter press used to dewater anaerobically digested sludge from Jones Island Water Reclamation Facility, Milwaukee, WI, was acquired to test the impact of a complex anaerobic wastewater matrix on the fate and impact of TCS, E2 and SMX during ion exchange-regeneration. Water quality parameters including pH, chemical oxygen demand (COD), total organic carbon (TOC), and total suspended solids

(TSS) were measured in accordance with standard methods [40], results of which are provided in SI 13. Ammonium-N content in the filtrate was approximately 110 mg/L; no additional N was added. Phosphate-P content in the effluent was approximately 1.4 mg/L; additional P was added for a final P concentration of 8 mg/L. Approximately 300 µg/L each of TCS, E2 and SMX stock solution was added to the anaerobic effluent (background concentrations were below detection). Each bottle was dosed with 5 g/L of clinoptilolite, 1 g/ of LayneRT, or 1 g/L of DOW-HFO-Cu, as described for the batch experiments. Controls were performed using no ion exchangers to investigate the adsorption of micropollutants to the organic carbon in the wastewater matrix. Samples were analyzed after four days to determine the extent of removal and desorption from the ion exchangers.

Struvite precipitation in the presence of micropollutants

Batch tests were conducted to determine the fate of micropollutants during struvite precipitation in Milli-Q water. A molar ratio of P:N:Mg=1:1:1 was targeted by mixing $Na_2HPO_4 \bullet 7H_2O$ (165 mL, 4.26 g/L), NH_4Cl (15 mL, 9.33 g/L), $MgCl_2 \bullet 6\ H_2O$ (20 mL, 26.65 g/L). Approximately 300 µg/L each of TCS, E2, and SMX was added. To mimic the regeneration brine, the pH was adjusted to 9 using NaOH and 2% NaCl was added. The solution was mixed on a shaker table at 180 rpm for 40 min and allowed to settle for 10 min [33]. Filtrate was collected before and after the precipitation reaction for quantification of micropollutants and nutrients.

Analytical methods

The standard phenate and ascorbic acid methods were used to quantify NH_4-N and PO_4-P, respectively [40]. Micropollutants were quantified via online solid-phase extraction (SPE, to eliminate interferences with micropollutant detection from background ions) with single quadrupole liquid chromatograph-mass spectrometry (LC-MS). An online SPE cartridge (Phenomenex, Torrance, CA, USA) was incorporated in the LC-MS system (LC-MS 2020, Shimadzu, Columbia, MD, USA). All samples were filtered through 0.45 µm PTFE filters. 13C-TCS, estrone (E1) and 13C-SMX were added as internal standards before SPE. Details of the SPE-LC-MS method are provided in the SI (S3). Method detection limits were 8 µg/L TCS, 8 µg/L E2, and 9 µg/L SMX. Recovery of TCS, E2, and SMX was between 70 – 130% [41].

Data analysis

Adsorption capacity from batch ion exchange tests and percent recovery from exchange-regeneration tests were calculated as described in the SI, Section S4. Nutrient removal kinetics were modelled as pseudo-second order reactions (which demonstrated the best fit for the data), as described in the SI (S5).

Isotherm modeling and statistical analysis (t-test, α level = 5%) were conducted using GraphPad Prism 6 (Graphpad Software, Inc., La Jolla, CA). To determine the relative influence of NaOH and NaCl on the recovery of NH_4-N, PO_4-P, or micropollutants during regeneration, response surface methodology (RSM) was used in R (S6) [42].

Results and Discussion

The impact of micropollutants on nutrient ion exchange reaction kinetics

The reaction rate of nutrient ion exchange with and without micropollutants was determined in batch studies. The nutrient ion exchange kinetics (Figure 1) were modeled as pseudo-second order reactions [43,44], which provided the best fit (average fitting parameters of linearized nutrient exchange kinetic curves are shown in Table S7 and equilibrium curves are shown in Figure S2). The presence of micropollutants significantly decreased ammonium and phosphate exchange reaction rate constants (Table 1, calculated using Eq. S5). When micropollutants were present in the water, the reaction rate constants for clinoptilolite, LayneRT and DOW-HFO-Cu decreased by 32%, 85% and 80%, respectively (S7, Figure S2).

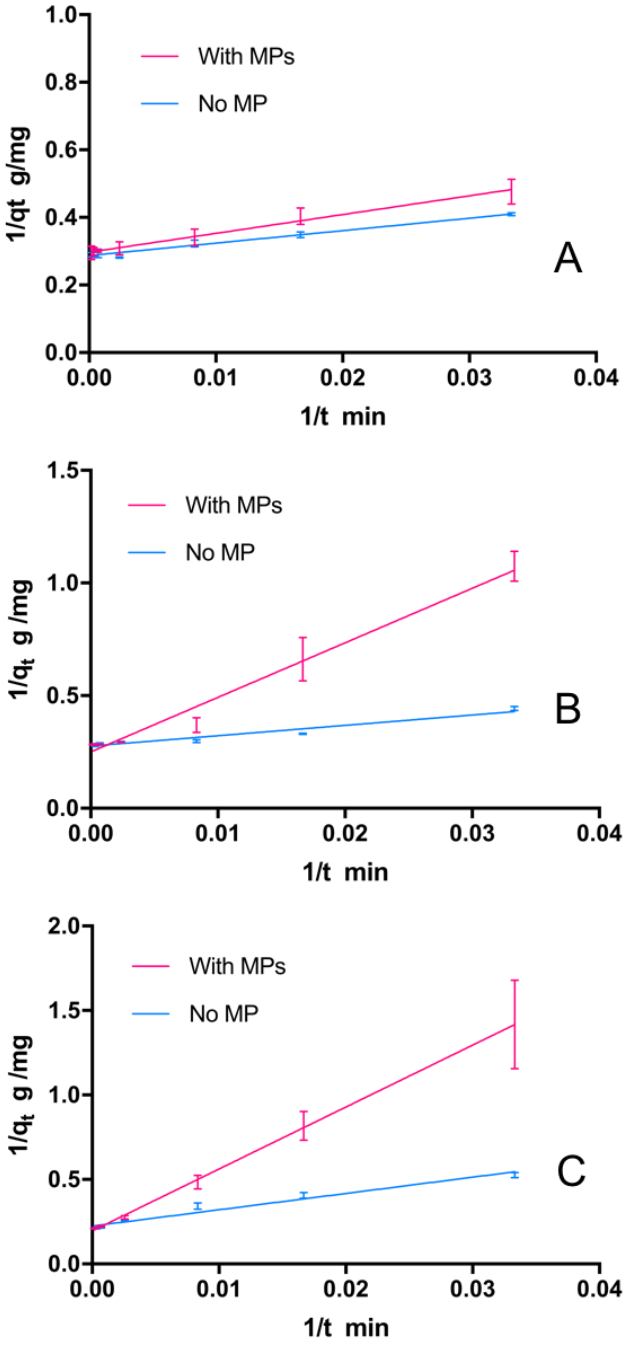

Figure 1: Linearized second order nutrient removal kinetics curves, plotted as the reciprocal of total adsorbed amount per unit mass of exchanger ($1/q_t$, g/mg) versus the reciprocal of time (1/t, 1/min). The plots show nutrient removal kinetics with and without micropollutants (MPs) for: A) NH_4-N removal by clinoptilolite, B) PO_4-P removal by LayneRT, and C) PO_4-P removal by DOW-HFO-Cu. The data points represent averages and error bars represent ± 1 standard deviation of triplicate experiments.

Table 1: Pseudo-second order reaction rate constants for nutrient ion exchange reactions with and without micropollutants

Nutrient	Ion Exchanger	Rate Constant	(L/mg/min)	p-value
		With Micropollutants	**Without Micropollutants**	
Ammonium	Clinoptilolite	0.015	0.022	0.0002
Phosphate	LayneRT	0.003	0.020	<0.0001
Phosphate	DOW-HFO-Cu	0.001	0.005	<0.0001

According to Planzinski et al. (2013), the pseudo-second order reaction model for spherical sorbent particles can be well interpreted in terms of an intraparticle diffusion model. This model assumes that the overall sorption reaction rate is controlled by the rate of sorbate diffusion across the sorbate/solution interface within pores [45]. In terms of nutrient exchange in this study, reductions in reaction rates in the presence of micropollutants may have been caused by the micropollutants interfering with nutrient diffusion from the aqueous phase to the solid surface of the adsorbent [46,47]. Although micropollutants significantly decreased nutrient ion exchange reaction rates, micropollutants did not impact the total amount of nutrients sorbed at equilibrium (Figure S2). The long-term effect of micropollutants on the suppression of nutrient ion exchange rates could potentially hinder the removal of nutrients by reducing the number of bed volumes treated prior to regeneration.

Adsorption of micropollutants onto nutrient ion exchangers

Batch studies were conducted to track the fate of micropollutants during nutrient removal via ion exchange. The three micropollutants were adsorbed to varying extents, as shown in Figure 2. LayneRT adsorbed 85.6±4.5% TCS, 64.4%±4.1 E2, and 51.6±8.0% SMX. DOW-HFO-Cu adsorbed 86.2±2.3% TCS, 88.2±4.6% E2, and 65.1±5.1% SMX. The extent of micropollutants adsorbed on each resin was proportional to the micropollutant log D_{ow} values (Table S1), as the most hydrophobic micropollutant, TCS, exhibited the greatest adsorption, while the most hydrophilic micropollutant, SMX, exhibited the least adsorption. Using clinoptilolite to capture ammonium, TCS and E2 were not readily adsorbed ($p=0.314$ for TCS and $p=0.067$ for E2), and the SMX concentration at the end of the equilibrium period did not differ significantly from the initial concentration ($p=0.154$), signifying that these micropollutants were not readily removed with clinoptilolite.

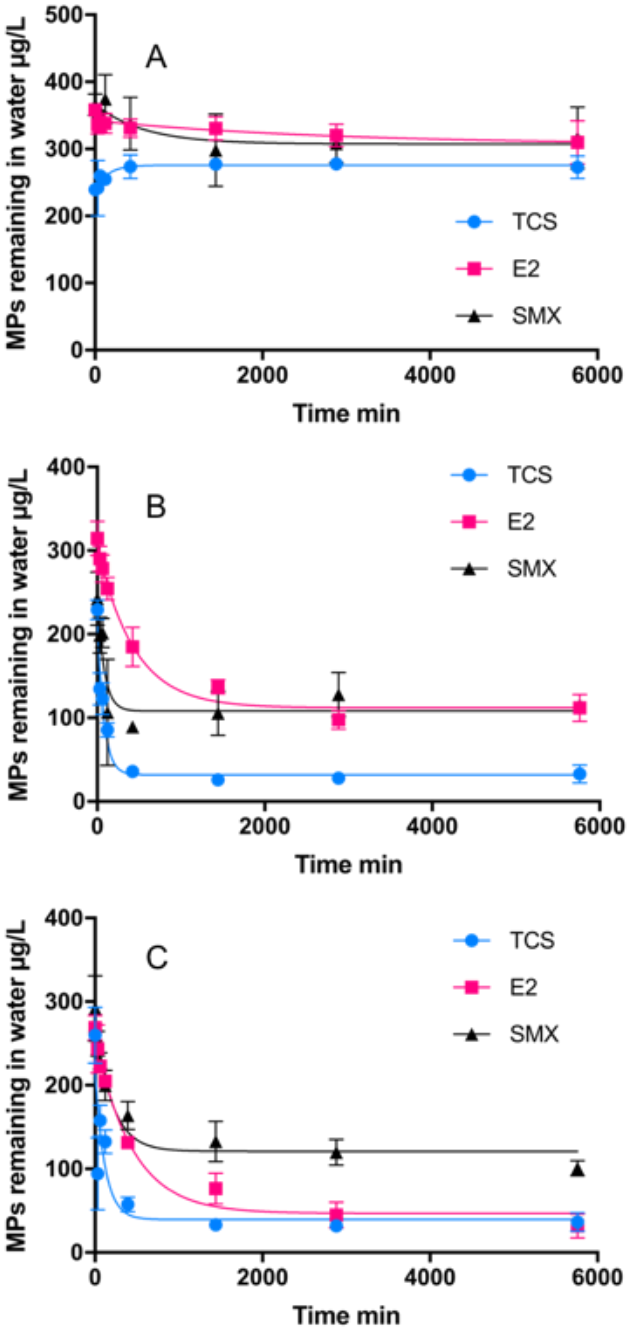

Figure 2: Micropollutant (MP) removal by three ion exchangers, A) clinoptilolite, B) LayneRT, and C) DOW-HFO-Cu, over time during batch tests. Feed water concentrations were ~300±50 µg/L each for TCS, E2, and SMX. Initial nutrient concentrations were 40 mg-N/L and 5 mg-P/L, with pH=7. The data points represent average results and error bars depict ± 1 standard deviation of triplicate experiments.

Clinoptilolite has a negative surface charge (S8, Figure S3), making it unlikely to adsorb the negatively charged dissociated fractions of TCS, E2, or SMX through coulombic attraction. Furthermore, according to pore size analysis, the mode pore width of clinoptilolite is 10.2 Å (S9, Figure S4). According to 3D-structure measurements in ChemDraw®, TCS has a minor dimension of 7.9 Å and a major dimension of 13.7 Å. The minor and major dimensions of E2 are 8.5 Å and 18 Å, respectively, while the minor and major dimensions of SMX are 14 Å and 15 Å, respectively. As the molecular size of the micropollutants is near or larger than the clinoptilolite pores, the likelihood for adsorption of micropollutants due to transport into pores is low [48]. Poor adsorption of SMX on clinoptilolite was also demonstrated previously [49].

On the other hand, the phosphate-selective exchange resins, LayneRT and DOW-HFO-Cu, readily sorbed TCS, E2, and SMX at neutral pH (Figures 2B and 2C, respectively). Gas sorption tests indicated that LayneRT has a mode pore size of 20.2 Å, and DOW-HFO-Cu has a mode pore size of 23.4 Å (Figure S4). Thus, the phosphate resins' pores are larger (in comparison to clinoptilolite's mode pore size of 10.2 Å) and more accessible for micropollutant adsorption.

There are two plausible means by which micropollutants could bind with phosphate-selective ion exchange resins: i) coulombic attraction due to opposite charges, and ii) non-coulombic attractions such as hydrophobic interactions, hydrogen bonding, and aromatic system π stacking [50–52]. Further discussion on mechanisms of micropollutant-ion exchanger interaction is provided in the *Potential mechanisms of micropollutant-ion exchanger interaction* section.

The impact of micropollutants on nutrient ion exchange capacity

Nutrient ion exchange isotherm modeling was performed using data from batch tests conducted with and without micropollutants in the feed water to assess micropollutants' influence on nutrient exchange capacity and mechanisms. Exchange of ammonium using clinoptilolite fit the empirical Langmuir isotherm model (Figure S5A), which assumes one solute ion per adsorption site, forming a single layer on the sorbate surface [53]. The ammonium exchange isotherms with and without micropollutants were not significantly different ($p=0.756$).

An empirical sigmoidal isotherm (type D) [54,55], provided the best fit for modeling exchange of phosphate via LayneRT and DOW-HFO-Cu resins with and without micropollutants in the feed water (Figures S5B and S5C). A sigmoidal isotherm often occurs when using a homogenous adsorbent [54], such as LayneRT and DOW-HFO-Cu resins, which are manufactured under controlled conditions. Observation using a

scanning electron microscope (Figure S6) together with surface pore analysis indicated that these phosphate ion exchangers were more homogeneous than clinoptilolite, reaffirming the underlying basis for the best fit isotherm model behaviors. At near-neutral pH, the predominant orthophosphate species, $H_2PO_4^-$ and HPO_4^{2-}, are Lewis bases (electron pair donors) that can exhibit strong ligand adsorption on the HFO in LayneRT resin, as well as on both HFO and Cu^{2+} in the DOW-HFO-Cu resin, by forming inner-sphere complexes through coordinate bonding. Sigmoidal isotherms provide good representations of this type of phosphate exchange, according to previous reports [29,36,56–58]. The inflection expected for a sigmoidal isotherm was not observed, likely due to the small phosphorus range tested (less than 5 mg/L).

Similar to the case for clinoptilolite, there was no significant difference in exchange capacity with and without micropollutants for the phosphate-selective resins (LayneRT p=0.768 and DOW-HFO-Cu p=0.796, Figure S5). Although the presence of micropollutants slowed the reaction rates of nutrient ion exchange, as described previously, the amount (q_e) of phosphate or ammonium exchanged at equilibrium remained similar with or without micropollutants, as did the shape of the isotherm. For clinoptilolite, the ammonium isotherm was not expected to change since TCS, E2 and SMX did not adsorb effectively (Figure 2A). For LayneRT and DOW-HFO-Cu, it is possible that the low initial concentrations of micropollutants relative to nutrients and different adsorption/exchange mechanisms contributed to the lack of observed change in the nutrient exchange isotherms with and without micropollutants.

Potential mechanisms of micropollutant-ion exchanger interaction

In near-neutral pH feed water, TCS and E2 are predominantly in the neutral form (88.8% neutral for TCS and 99.9% for E2, Figure S1). Therefore, the non-coulombic mechanisms for TCS and E2 adsorption by LayneRT and DOW-HFO-Cu differ from the electrostatic mechanism that controls phosphate exchange. The aromatic pyridyl group in the bis-picolylamine attached to the DOWEX M4195 polymer matrix, and the benzene ring of LayneRT's backbone structure, are able to form π stacking with the benzene rings on TCS and E2 molecules [39,59].

Negatively charged dissociated SMX is more likely to adsorb to LayneRT and DOW-HFO-Cu via coulombic attraction with positively charged moieties that are dissociated while in water (Figure S3). At pH 7, the majority of SMX molecules are anionic (98.0%) (Figure S1), implying that the adsorption onto phosphate exchangers is likely due to coulombic attraction. Ionic SMX may be adsorbed to the quaternary ammonium groups (R_4N^+) on LayneRT's surface via coulombic attraction. The removal of ionic SMX by DOW-HFO-Cu may be attributed to the coulombic attraction between the ions and chelated HFO or

Cu^{2+} that forms outer sphere complexes [36]. Additionally, the π-electron rich moiety in SMX's structure may form π stacking with the ion exchanger surface, which may play a minor role. Alternately, phosphate prefers ligand adsorption by forming inner sphere complexes via both coulombic and Lewis acid-base attraction with HFO [36,60]. In accordance with these potentially different adsorption mechanisms and low micropollutant loadings, ionic SMX is unlikely to compete with phosphate for exchange sites on LayneRT and DOW-HFO-Cu resins. However, the absence of an inflection point in the phosphate exchange isotherm indicates that the functional HFO and Cu^{2+} sites are far from saturation. Considering the initial concentrations of TCS, E2 and SMX (approximately 0.0012 mM, whereas phosphate was 0.16 mM), the availability of binding sites on the resins was sufficient for phosphate adsorption.

The impact and fate of micropollutants during ion exchange regeneration

Ion exchange regeneration was performed to investigate the fate of the micropollutants adsorbed on the ion exchangers, and their potential effect on nutrient desorption during regeneration. Following ion exchange, regeneration brine containing varying concentrations of NaCl and NaOH was used to increase adsorption capacity of exhausted clinoptilolite, LayneRT, and DOW-HFO-Cu [61]. Micropollutants that were adsorbed onto phosphate exchangers did not impact nutrient desorption, as shown in Figure 3 ($p=0.058$ for LayneRT and $p=0.699$ for DOW-HFO-Cu). Since micropollutants were not adsorbed by clinoptilolite during the ion exchange stage, micropollutants did not have a significant impact on the desorption of ammonium ($p=0.57$). Therefore, clinoptilolite was not considered in further studies of micropollutant desorption during regeneration.

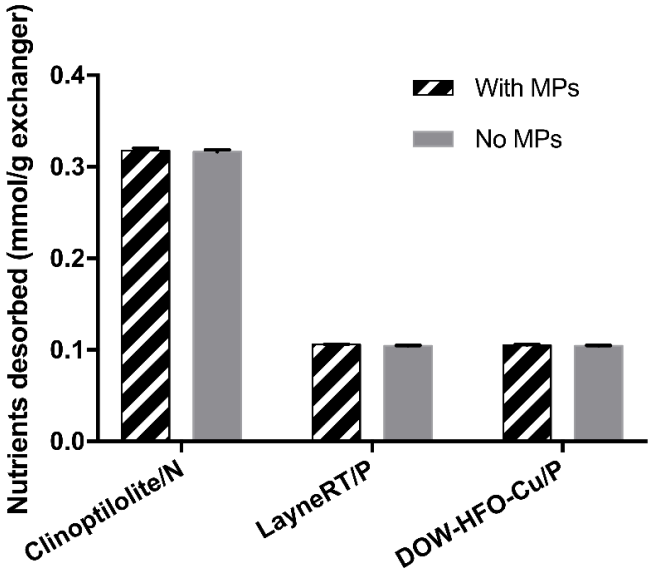

Figure 3. Nutrient desorption per mass of ion exchanger during ion exchange-regeneration batch tests, with and without micropollutants (MPs, ~300 µg/L each TCS, E2, and SMX, in the pH=7 ion exchange feed waters). The regeneration brine for phosphate exchangers was 2% NaOH + 2% NaCl and was 8% NaCl for clinoptilolite. The data represent average results and error bars show ± 1 standard deviation of triplicate experiments.

To explore the impact of NaCl and NaOH on micropollutant desorption from LayneRT and DOW-HFO-Cu resins, concentrations of NaCl and NaOH in the regenerant were varied, as listed in Tables S2-S5. There was no significant correlation between regeneration brine constituents and micropollutant desorption ($p>0.05$), except for NaOH, which yielded significant positive linear correlations with SMX ($p=0.05$, $\beta_1=26.95$) and TCS ($p=0.032$, $\beta_1=12.31$) for desorption from DOW-HFO-Cu. Under the tested conditions, micropollutant desorption from LayneRT or DOW-HFO-Cu cannot be accurately predicted using the concentration of constituents in the regeneration brine, nor is it easy to control desorption by varying brine concentration, possibly due to the complexity of micropollutants' binding with ion exchangers. Therefore, the potential desorption of micropollutants is unlikely to influence the selection of regeneration brine in real-life operations. Instead, impacts on nutrient ion exchange capacity and operation costs will be the most important criteria when selecting a regenerant [62].

Although there was no significant correlation between regeneration brine concentration and micropollutant desorption, the extent of desorption (based on percent mass desorbed relative to initial mass sorbed) varied among the micropollutants (Figure 4). The variations in the extent of SMX desorption indicate that the main mechanisms of SMX adhesion to ion exchangers may be coulombic attraction, which is more easily disturbed by high ionic strength solution compared to non-columbic attractions. Comparing data in Figures 2 and 4, micropollutant desorption was inversely related with the degree of adsorption, where compounds that poorly adsorbed were better desorbed (i.e., SMX). For TCS, the extent of adsorption (Fig. 2) and desorption (Fig. 4) onto the two phosphate exchangers was similar. For E2, adsorption using LayneRT was lower than for DOW-HFO-Cu (Figure 2), and desorption was generally higher than DOW-HFO-Cu (Figure 4), which indicates that E2 has stronger binding with LayneRT than DOW-HFO-Cu.

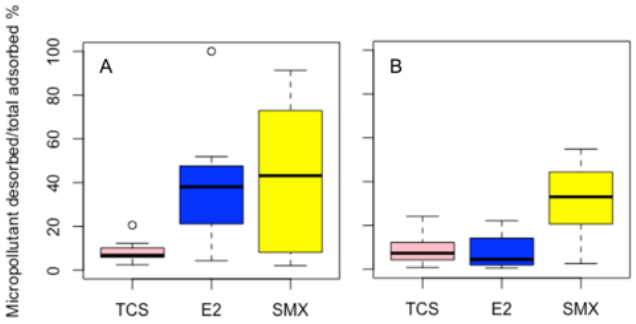

Figure 4. Micropollutant desorption relative to total adsorption for batch ion exchange-regeneration tests with varying NaCl and NaOH regenerant compositions using A) LayneRT and B) DOW-HFO-Cu resin (n = 11 for each exchanger). Clinoptilolite is not shown because no significant adsorption was observed. The horizontal bold line indicates the median. The boxes represent the first and third quartile of the data set. The whiskers above and below the boxes show the locations of the minimum and maximum. The hollow circles signify outliers.

Phosphate readily desorbed from each phosphate exchanger under the regeneration conditions tested, but desorption did not correlate to NaCl or NaOH concentration ($p=0.791$ for LayneRT and $p=0.380$ for DOW-HFO-Cu, first order linear regression model; Tables S2 and S4). Phosphate desorption was 3.50±0.19 mg-P/g LayneRT (94.5±5.54% of the portion captured was released) and 3.69±0.30 mg-P/g DOW-HFO-Cu (74.35±5.31%). The mass of phosphate desorbed from LayneRT was not significantly different from that desorbed from DOW-HFO-Cu ($p=0.12$). However, DOW-HFO-Cu resin generally demonstrated greater total mass removal of phosphate, possibly indicating stronger binding.

Phosphate ions are exchanged by forming inner-sphere complexes with HFO and Cu^{2+} on the exchangers via coulombic and Lewis acid-base interactions, while adsorption of SMX in pH 7 feed water was possibly due to non-selective coulombic attraction forming outer sphere complexes [36]. Thus, the attachment of both phosphate and SMX to phosphate exchange resins was likely due to electrostatic attractions, which would be easily disrupted by the concentrated Cl^- and OH^- in the regeneration brine [60]. As noted previously, adsorption of TCS and E2 to the two phosphate exchange resins was not likely due to coulombic attraction, indicating that the presence of strong counter ions would not significantly affect desorption [60].

Desorption of TCS, E2, and SMX (median <50%) was much lower than phosphorus desorption (>90%). These results indicate that the majority of the micropollutants

tended to irreversibly adsorb to the ion exchangers, regardless of the interactions between micropollutants and exchangers (e.g., coulombic or non-coulombic). Landry and Boyer [60] also reported low desorption of diclofenac sorbed on polymeric strong-base anion exchange resins (24% using 4% NaCl brine). Even though coulombic forces played a major role for diclofenac (pKa= 4.7) attaching to the polystyrene resin in fresh urine (pH = 6), high strength regeneration brine could not disrupt the interaction between the dissociated diclofenac and the resin [60]. Previous studies have also shown favorable adsorption of chlorinated phenols and aromatic micropollutant anions on polymeric exchangers, with a preference for these contaminants over inorganic chloride ions present in either feed water or regeneration solutions [63,64]. This was attributed to the non-polar moiety of the aromatic ions leading to simultaneous hydrophobic interactions and coulombic attractions [65].

The low desorption to adsorption ratio of micropollutants from ion exchangers potentially introduces additional concerns for flow-through reactor operation. Based on the lack of effective micropollutant desorption during regeneration, over time, ion exchangers may become saturated with adsorbed micropollutants. Consequently, micropollutants in the influent may eventually bypass the ion exchange bed, and be carried into the ion exchange effluent. During WRRF operation, the ion exchange effluent would either be recycled to the head of the WRRF or discharged to receiving water, depending on whether the ion exchange feed water was from an AD or AnMBR . Moreover, it is unknown if a buildup of micropollutants on ion exchangers due to inefficient desorption would eventually block nutrient exchange sites. In this study, the adsorption of micropollutants (present at low concentrations in the feed water) on ion exchangers had negligible impact on nutrient removal, but long-term performance is uncertain.

The impact and fate of TCS, E2 and SMX during nutrient ion exchange-regeneration in actual anaerobic filtrate

Ion exchangers were tested in anaerobic filtrate supplemented with 300 µg/L each TCS, E2, and SMX to investigate the impact of micropollutants on nutrient exchange in a real wastewater matrix containing organic carbon (water quality parameters are listed in SI, Table S9). The presence of micropollutants in actual anaerobic wastewater did not impact nutrient removal or regeneration (all t-test p-values were greater than 0.05; Table 2), this finding was similar to the finding from Milli-Q water tests. Compared to other constituents in real anaerobic filtrate, such as organic carbon and ions, micropollutants were in much lower levels, and therefore, they less likely had substantial impact on nutrient removal.

Table 2: Nutrient removal and regeneration by ion exchangers in anaerobic effluent, with and without the presence of micropollutants. All tests were conducted in triplicate, and values shown indicate means ± 1 standard deviation.

Ion exchanger	Nutrient mole		No MP	With MPs	p-value
Clinoptilolite	NH_4-N mmol/g exchanger	removed	0.69±0.07	0.58±0.15	0.31
		regenerated	0.69±0.07	0.48±0.08	0.31
LayneRT	PO_4-P mmol/g exchanger	removed	0.13±0.00	0.13±0.00	0.97
		regenerated	0.11±0.00	0.10±0.00	0.10
DOW-HFO-Cu		removed	0.13±0.00	0.12±0.00	0.09
		regenerated	0.11±0.01	0.11±0.00	0.09

The adsorption and desorption of micropollutants during nutrient ion exchange-regeneration was changed in complex wastewater matrix compared to pure water tests. In control experiments without ion-exchangers, approximately 44% of TCS (the most hydrophobic compound) was lost to the wastewater matrix, and approximately 26% of E2 was lost to the matrix. The most hydrophilic compound tested, SMX, was not lost to the wastewater matrix. Therefore, when calculating percent removal by ion exchangers, the compound lost in control tests was considered. In experiments conducted with ion exchangers, as shown in Table 3, the extent of SMX adsorption onto phosphate exchangers from anaerobic filtrate was 57%, which was similar to the results from MilliQ water tests, indicating suspended solids and organic matter did not interfere with SMX adsorption. However, SMX percent desorption decreased in real effluent tests. TCS and E2 adsorption onto ion exchangers from real anaerobic filtrate decreased in the complex matrix compared with previous pure water tests, which could be attributed to adsorption onto suspended solids and competition from organic carbon with these neutral micropollutant molecules. The extent of TCS and E2 desorption were much higher in the anaerobic filtrate than in pure water tests. These results indicate that constituents in real anaerobic wastewater would hinder TCS and E2 adsorption and desorption with phosphate exchangers.

Table 3: TCS, E2 and SMX removal and regeneration by ion exchangers in anaerobic effluent.

	Clinoptilolite		LayneRT		DOW-HFO-Cu	
	% removal	% regeneration	% removal	% regeneration	% removal	% regeneration
TCS	NA	NA	50	74	54	68
E2	NA	NA	59	55	66	68
SMX	NA	NA	57	3	71	4

The fate of micropollutants during struvite precipitation

The concentrations of TCS, E2 and SMX in the aqueous solution did not decrease during struvite precipitation (Table S8), indicating that these micropollutants were not able to adsorb on, or assimilate into, struvite crystals. The distribution coefficient D_{ow} (Table S1) shows that, at pH 9, which was used for struvite precipitation, the majority of TCS and E2 molecules were still hydrophobic, whereas SMX was mostly dissociated and hydrophilic. Previous reports suggested that the accumulation of micropollutants in struvite cannot be fully explained by hydrophobicity since relatively hydrophilic compounds tetracycline (log K_{ow} = -1.37) and quinolones (log K_{ow} = 0.89) were observed in struvite crystals [34,35].

In previous studies, the majority of tetracycline accumulation in struvite was considered to be due to spontaneous assimilation into struvite's structure during formation, rather than being adsorbed onto the surface of pre-formed struvite [34,35]. This finding was explained by tetracycline's potential as a ligand, wherein the molecule's β-hydroxyl ketone moiety can donate electron pairs to form stable complexes with Mg^{2+} or Ca^{2+} [35,66–68]. Thus, the partitioning of E2, TCS, and SMX to the aqueous phase observed in this study may be explained by the compounds' inability to form coordination complexes with Mg^{2+} in struvite. According to the pKa value, more than 98% of E2 was in neutral form at pH 9, clearly preventing it from participating in Lewis acid-base reactions with metal ions. For TCS, the charged fractions dominate at pH 9. The dissociated phenolic group on TCS (Table S1) is affected by resonance due to the presence of benzene. The resonance phenomenon makes non-bonded electron pairs of oxygen form double bonds with benzene carbon, turning the dissociated phenolic group into more acidic forms, which can result in difficulty forming a coordinate bond between TCS and Mg^{2+} [37,69]. Dissociated SMX also dominates at pH 9. The charged fraction of SMX can form coordinate complexes with first and second row transition metals such as Cr, Mn(II), Zn(II), Cd(II), and Co(II).[70,71] However, as negligible removal of SMX was observed during struvite precipitation, SMX may not be able to form complexes with metals such as

Mg(II). According to hard soft acid bases rules [72], Mg is a hard acid that is relatively nonpolarizable; therefore, it is easier for Mg to form stable complexes with hard bases such as OH^-, which is present in tetracyclines. However, it is more difficult for Mg to form stable complexes with the soft base functional groups in SMX such as sulfonamide nitrogen, amino nitrogen, and sulfonyl oxygen. Thus, micropollutants that cannot form coordinate complexes with the metal in struvite are unlikely to be present in precipitated struvite.

Conclusions

This research demonstrated that ion exchange-precipitation can effectively recover nutrients from nutrient-rich waters (both lab-grade and actual anaerobic effluent), regardless of the presence of TCS, E2 and SMX. The extent of nutrient sorption and desorption was not influenced by the presence of these micropollutants, but the reaction rate of nutrient exchange decreased when TCS, E2, and SMX were present. These neutral and anionic micropollutants were able to co-adsorb to phosphate exchangers while orthophosphate was exchanged and were desorbed during ion exchanger regeneration. However, these micropollutants did not partition to precipitated struvite, so they do not pose risks in the final solid fertilizer product.

The findings from this research have real-world implications. Specifically, the adsorption/desorption behaviors indicated that micropollutants could accumulate on ion exchangers, which may eventually lead to saturation of the ion exchangers, causing bypass of micropollutants into the ion exchange effluent that would put additional stress on mainstream treatment or receiving natural waters, depending on whether ion exchange feed water is from AnMBRs or AD belt filter filtrate. When the micropollutants were present in actual anaerobic wastewater, they did not interfere with nutrient removal and recovery; however, the complex matrix of anaerobic wastewater tended to decrease co-adsorption and increase desorption of TCS and E2 from phosphate-specific exchangers. There could also be greater chances for these neutral compounds to be present in the ion exchange bed effluent or regeneration solution. Therefore, other non-selective adsorbents, such as biosolids-derived biochar, could be employed prior to ion exchange to remove micropollutants before recovering nutrients [52].

The fate of micropollutants through ion exchange-precipitation process is closely related to the physical and chemical properties of both micropollutants, ion exchangers and struvite. For example, clinoptilolite did not sorb selected micropollutants, likely on the basis of surface charge and molecular size disparities, and the ability of micropollutants to form coordinate complexes with the metal ions in struvite crystals appears to be the key factor that determines partitioning of micropollutants between the aqueous phase

and the precipitated struvite product. Future research extending these results to cationic and zwitterionic micropollutants can help to derive more universal conclusions related to the impact and fate of micropollutants during nutrient recovery.

Supporting Information

The Supporting Information (SI) is available free of charge on the RSC Publishing Home website. The SI includes additional information related the micropollutant structure and properties, desorption datasets, LC-MS operation and analysis, calculation details of adsorption capacities and recoveries, kinetic modeling approach, response surface methodology, kinetic datasets, activity coefficient calculations, zeta potential and pore size analyses, nutrient isotherms, SEM images, and struvite data.

Acknowledgements

This study was funded by a grant from the Lafferty Family Foundation. Y.T. was partially supported by Marquette University's Jobling Fellowship. The authors greatly appreciate assistance from Dr. Silva at University of Wisconsin-Milwaukee for her help with ion exchanger pore volume analysis.

References

1 D. E. Carey, Y. Yang, P. J. McNamara and B. K. Mayer, *Bioresour. Technol.*, 2016, **215**, 186–198.

2 M. D. Seib, K. J. Berg and D. H. Zitomer, *Environ. Sci. Water Res. Technol.*, 2016, **2**, 290–297.

3 P. L. McCarty, J. Bae and J. Kim, *Environ. Sci. Technol.*, 2011, **45**, 7100–6.

4 A. L. Smith, L. B. Stadler, L. Cao, N. G. Love, L. Raskin and S. J. Skerlos, *Environ. Sci. Technol.*, 2014, **48**, 5972–5981.

5 J. Jimenez, E. Latrille, J. Harmand, A. Robles, J. Ferrer, D. Gaida, C. Wolf, F. Mairet, O. Bernard, V. Alcaraz-Gonzalez, H. Mendez-Acosta, D. Zitomer, D. Totzke, H. Spanjers, F. Jacobi, A. Guwy, R. Dinsdale, G. Premier, S. Mazhegrane, G. Ruiz-Filippi, A. Seco, T. Ribeiro, A. Pauss and J.-P. Steyer, *Rev. Environ. Sci. Bio/Technology*, 2015, **14**, 615–648.

6 Wisconsin DNR, *Effluent Standards And Limitations For Phosphorus*, US, 2010.

7 B. K. Mayer, D. Gerrity, B. E. Rittmann, D. Reisinger and S. Brandt-Williams, *Crit. Rev. Environ. Sci. Technol.*, 2013, **43**, 409–441.

8 B. E. Rittmann, B. Mayer, P. Westerhoff and M. Edwards, *Chemosphere*, 2011, **84**,

846–853.
9 T. S. S. Neset and D. Cordell, *J. Sci. Food Agric.*, 2012, **92**, 2–6.
10 V. Smill and R. A. Streatfeild, *Electron. Green J.*, 2002.
11 B. K. Mayer, L. A. Baker, T. H. Boyer, P. Drechsel, M. Gifford, M. A. Hanjra, P. Parameswaran, J. Stoltzfus, P. Westerhoff and B. E. Rittmann, *Environ. Sci. Technol.*, 2016, **50**, 6606–6620.
12 B. D. Blair, J. P. Crago, C. J. Hedman, R. J. F. Treguer, C. Magruder, L. S. Royer and R. D. Klaper, *Sci. Total Environ.*, 2013, **444**, 515–21.
13 D. E. Carey, D. H. Zitomer, A. D. Kappell, M. J. Choi, K. R. Hristova and P. J. McNamara, *Environ. Sci. Process. Impacts*, 2016, **18**, 1060–1067.
14 D. E. Carey and P. J. Mcnamara, *Front. Microbiol.* , 2015, 5.
15 P. J. McNamara, T. M. Lapara and P. J. Novak, *Environ. Sci. Technol.*, 2014, **48**, 7393–7400.
16 D. E. Carey and P. J. McNamara, *Chemosphere*, 2016, **163**, 22–26.
17 A. M. Vajda, L. B. Barber, J. L. Gray, E. M. Lopez, J. D. Woodling and D. O. Norris, *Environ. Sci. Technol.*, 2008, **42**, 3407–3414.
18 K. Hruska and M. Franek, *Vet Med*, 2012, **57**, 1–35.
19 J. C. Underwood, R. W. Harvey, D. W. Metge, D. A. Repert, L. K. Baumgartner, R. L. Smith, T. M. Roane and L. B. Barber, *Environ. Sci. Technol.*, 2011, **45**, 3096–3101.
20 V. G. Samaras, A. S. Stasinakis, D. Mamais, N. S. Thomaidis and T. D. Lekkas, *J. Hazard. Mater.*, 2013, **244**, 259–267.
21 T. Z. D. de Mes, K. Kujawa-Roeleveld, G. Zeeman and G. Lettinga, *Water Sci. Technol.*, 2008, **57**, 1177–1182.
22 J. Malmborg and J. Magnér, *J. Environ. Manage.*, 2015, **153**, 1–10.
23 V. M. Monsalvo, J. A. McDonald, S. J. Khan and P. Le-Clech, *Water Res.*, 2014, **49**, 103–112.
24 T. Alvarino, S. Suarez, J. M. Lema and F. Omil, *J. Hazard. Mater.*, 2014, **278**, 506–513.
25 L. Gonzalez-Gil, M. Papa, D. Feretti, E. Ceretti, G. Mazzoleni, N. Steimberg, R. Pedrazzani, G. Bertanza, J. M. Lema and M. Carballa, *Water Res.*, 2016, **102**, 211–220.
26 A. Hedström, *J. Environ. Eng.*, 2001, **127**, 673–681.
27 M. Razali, Y. Zhao and M. Bruen, *Sep. Purif. Technol.*, 2007, **55**, 300–306.
28 D. Zhao and A. K. Sengupta, *Water Res.*, 1998, **32**, 1613–1625.

29 S. Sengupta and A. Pandit, *Water Res.*, 2011, **45**, 3318–30.
30 R. Laridi, J. C. Auclair and H. Benmoussa, *Environ. Technol.*, 2005, **26**, 525–536.
31 J. A. O'Neal and T. H. Boyer, *Environ. Sci. Water Res. Technol.*, 2015, **1**, 481–492.
32 E. V Münch and K. Barr, *Water Res.*, 2001, **35**, 151–159.
33 A. T. Williams, D. H. Zitomer and B. K. Mayer, *Environ. Sci. Water Res. Technol.*, 2015, **1**, 832–838.
34 D. Antakyal, B. Kuch, V. Preyl and H. Steinmetz, *Proc. Water Environ. Fed.*, 2011, **2011**, 575–582.
35 S. Başakçilardan-Kabakci, A. Thompson, E. Cartmell and K. Le Corre, *Water Environ. Res.*, 2007, **79**, 2551–2556.
36 L. M. Blaney, S. Cinar and A. K. SenGupta, *Water Res.*, 2007, **41**, 1603–1613.
37 R. P. Schwarzenbach, P. M. Gschwend and D. M. Imboden, *Environmental organic chemistry*, John Wiley & Sons, 2005.
38 G. M. Lunn, L. E. Spencer, A. M. J. Ruby and A. McCaskill, 44th International Conference on Environmental Systems, 2014.
39 S. Sengupta and A. Pandit, *Water Res.*, 2011, **45**, 3318–3330.
40 APHA, AWWA and WEF, *Standard methods for the examination of water and wastewater*, 1998.
41 G. A. Smith, A. D. Zaffurio, M. L. Zimmerman and D. J. Munch, *Determination of Hormones in Drinking Water by Solids Phase Extraction (SPE)and Liquid Chromatography Electrospray Ionization Tandem Mass Spectrometry (LC-ESI-MS/MS)*, 2010.
42 D. C. Montgomery, *Applied statistics and probability for engineers third edition*, 2003, vol. 37.
43 Y. S. Ho and G. McKay, *Process Biochem.*, 1999, **34**, 451–465.
44 Y. S. Ho, *Water Res.*, 2006, 40, 119–125.
45 W. Plazinski, J. Dziuba and W. Rudzinski, *Adsorption*, 2013, **19**, 1055–1064.
46 R. Klaewkla, M. Arend and W. F. Hoelderich, in *Mass Transfer - Advanced Aspects*, 2011, pp. 667–684.
47 C. N. Sawyer, P. L. McCarty and G. F. Parkin, 2003.
48 S. D. Faust and O. M. Aly, *Chemistry of water treatment*, CRC Press, 1998.
49 T. Farí, A. R. Ruiz-Salvador and A. Rivera, *Microporous Mesoporous Mater.*, 2003, **61**, 117–125.
50 M. Carmona, A. De Lucas, J. L. Valverde, B. Velasco and J. F. Rodríguez, *Chem. Eng.*

J., 2006, **117**, 155–160.
51 M. Inyang and E. Dickenson, *Chemosphere*, 2015, **134**, 232–240.
52 Y. Tong, B. K. Mayer and P. J. McNamara, *Environ. Sci. Water Res. Technol.*, 2016, **2**, 761–768.
53 A. A. Halim, H. A. Aziz, M. A. M. Johari and K. S. Ariffin, *Desalination*, 2010, **262**, 31–35.
54 H.-J. Butt, K. Graf and M. Kappl, *Physics and chemistry of interfaces*, John Wiley & Sons, 2006.
55 G. Limousin, J.-P. Gaudet, L. Charlet, S. Szenknect, V. Barthès and M. Krimissa, *Appl. Geochemistry*, 2007, **22**, 249–275.
56 L. Cumbal and A. K. Sengupta, *Environ. Sci. Technol.*, 2005, **39**, 6508–6515.
57 C. Hinz, *Geoderma*, 2001, **99**, 225–243.
58 G. Limousin, J. P. Gaudet, L. Charlet, S. Szenknect, V. Barthès and M. Krimissa, *Appl. Geochemistry*, 2007, **22**, 249–275.
59 C. Janiak, *J. Chem. Soc. Dalt. Trans.*, 2000, 3885–3896.
60 K. A. Landry and T. H. Boyer, *Water Res.*, 2013, **47**, 6432–6444.
61 J. C. Crittenden, R. R. Trussell, D. W. Hand, K. J. Howe and G. Tchobanoglous, *MWH's water treatment: principles and design*, John Wiley & Sons, 2012.
62 N. P. Cheremisinoff, *Handbook of water and wastewater treatment technologies*, 2002.
63 K.-C. Lee and Y. Ku, *Sep. Sci. Technol.*, 1996, **31**, 2557–2577.
64 R. L. Hinrichs and V. L. Snoeyink, *Water Res.*, 1976, **10**, 79–87.
65 P. Li and A. K. SenGupta, *Environ. Sci. Technol.*, 1998, **32**, 3756–3766.
66 J. Tolls, *Environ. Sci. Technol.*, 2001, **35**, 3397–3406.
67 I. Turel, *Coord. Chem. Rev.*, 2002, **232**, 27–47.
68 M. O. Schmitt and S. Schneider, *PhysChemComm*, 2000, **3**, 42–55.
69 J. DeRuiter, .
70 G. Kanagaraj and G. N. Rao, *Synth. React. Inorganic, Met. Nano-Metal Chem.*, 1992, **22**, 559–574.
71 B. Kesimli and A. Topacli, *Spectrochim. Acta Part A Mol. Biomol. Spectrosc.*, 2001, **57**, 1031–1036.
72 R. G. Pearson, *J. Am. Chem. Soc.*, 1963, **85**, 3533–3539.